

Published in final edited form as:

Circ Res. 2014 February 14; 114(4): 660–671. doi:10.1161/CIRCRESAHA.114.302931.

Congenetic Fine-Mapping Identifies a Major Causal Locus for Variation in the Native Collateral Circulation and Ischemic Injury in Brain and Lower Extremity

Robert Sealock¹, Hua Zhang^{1,3}, Jennifer L. Lucitti^{1,3}, Scott M. Moore², and James E. Faber^{1,3}

¹Department of Cell Biology and Physiology, University of North Carolina at Chapel Hill

²Department of Surgery, University of North Carolina at Chapel Hill

³The McAllister Heart Institute, School of Medicine, University of North Carolina at Chapel Hill

Abstract

Rationale—Severity of tissue injury in occlusive disease is dependent on the extent (number and diameter) of collateral vessels, which varies widely among healthy mice and humans. However, the causative genetic elements are unknown. Recently, much of the variation among different mouse strains, including C57Bl/6J (B6, high extent) and BALB/cByJ (Bc, low), was linked to a QTL on chromosome 7 (*Candq1*).

Objective—We used congenic mapping to refine *Candq1* and its candidate genes and create an “isogenic” strain-set with large differences in collateral extent to assess their and *Candq1*'s impact, alone, on ischemic injury.

Methods and Results—Six congenic strains possessing portions of *Candq1* introgressed from B6 into Bc were generated and phenotyped. *Candq1* was refined from 27 to 0.737 Mb with full retention of effect, ie, return/rescue of phenotypes from the poor values in Bc to nearly those of wildtype B6 in the B6/B6 congenic mice: 83% rescue of low pial collateral extent, and 4.5-fold increase in blood flow and 85% reduction of infarct volume after middle cerebral artery occlusion; 54% rescue of low skeletal muscle collaterals, and augmented recovery of perfusion (83%) and function after femoral artery ligation. Gene deletion and *in-silico* analysis further delineated the candidate genes.

Conclusion—We have significantly refined *Candq1* (now designated Determinant of collateral extent-1, *Dce1*), demonstrated that genetic background-dependent variation in collaterals is a major factor underlying differences in ischemic tissue injury, and generated a congenic strain-set with wide, allele-dose-dependent variation in collateral extent for use in investigations of the collateral circulation.

Keywords

Collateral circulation; ischemic stroke; peripheral vascular disease; stroke genetics; mouse strain; cerebrovascular disease/stroke; genetics; animal models; physiology/pathophysiology

Address correspondence to: Dr. James E. Faber, Department of Cell Biology and Physiology, 111 Mason Farm Road, MBRB 5312, University of North Carolina, Chapel Hill, NC 24599, Tel: 919-966-0327, Fax: 919-966-6927, jefaber@med.unc.edu.

DISCLOSURES

None.

INTRODUCTION

Cerebral vascular disease, stroke, coronary artery disease (CAD), peripheral artery disease (PAD) and other obstructive arterial diseases are the leading cause of morbidity and mortality worldwide.¹ The extent (number and diameter) of native (pre-existing) collaterals, a unique type of blood vessel within the microcirculation of most tissues, plays a major role in reducing the severity of ischemic tissue injury and cell death. Collaterals are arteriole-to-arteriole anastomoses that cross-connect a small percentage of the outer branches of adjacent arterial trees.^{2,3} When the trunk of one of the trees becomes obstructed, collateral flow from the adjacent tree provides retrograde perfusion of the occluded tree. Even a modest amount of collateral flow can significantly decrease tissue injury after acute obstruction. Moreover, chronic obstruction induces collaterals to increase their anatomic lumen diameter, ie, remodel, by as much as 10-fold over days-to weeks, depending on the tissue and species. Collateral remodeling (arteriogenesis), which is stimulated by fluid shear stress, is capable of further greatly increasing collateral flow, depending on the extent of the native collaterals in the affected tissue and vigor of the molecular mechanisms that drive the remodeling process.

It is well known among stroke and neurovascular specialists, interventional cardiologists and vascular surgeons that tissue ischemia and infarction vary greatly among patients despite similar sites and severity of acute or chronic arterial obstruction. The mechanisms responsible for this variation remain ill-defined. Recent studies have reported wide variation among “healthy” individuals (ie, without obstructive disease in the tissue under examination) in the amount of blood flow provided by the native collateral circulation. In individuals without angiographically detectable CAD, ie, free of collateral remodeling that could differ and prevent interpretation of such measurements *vis-à-vis* native collateral extent, collateral flow index (CFI) was distributed normally and varied by ~10-fold, with 20% of individuals having low CFIs.⁴ Importantly, patients with CAD and poor collateral flows had a 64% higher risk of mortality.⁵ CFI also varied significantly in the lower extremities of individuals without PAD.⁶ And similarly, in patients with sudden thromboembolic occlusion of the middle cerebral artery (MCA) (the most common cause of ischemic stroke), retrograde perfusion of the MCA tree—as assessed by neuroimaging during the hyper-acute phase of stroke—varied widely, with 20% having poor pial collateral scores.^{7–11} Notably, such individuals sustain significantly larger infarct volumes, respond poorly to thrombolytic treatments, have increased risk for and severity of cerebral hemorrhage, and suffer increased morbidity and mortality.^{7–14} Thus, collateral score is increasingly being viewed as important diagnostic measurement to identify the optimal course of treatment and assess prognosis for recovery.^{12–14}

Nothing is known about the genetic and little about the environmental^{15–17} mechanisms that are responsible for the wide variation in native collateral-dependent flow in humans. However, recent studies in mice have found that genetic background is a major factor. In the brain, pial collateral number and diameter varied by 35-fold and 4-fold, respectively, among 21 inbred strains.^{18,19} Collateral number and diameter were highly heritable, positively correlated, and independent of potentially confounding variables (cerebral artery tree area, cortical area, body weight). Similarly wide variation in collateral extent was seen in other tissues of a subset of these strains, including hindlimb skeletal muscle.^{20,21} A genome-wide linkage analysis of an F2 cross between two strains at the extremes of the distribution for pial collateral number, C57Bl/6J (B6) and BALB/cByJ (Bc), yielded a single QTL on chromosome 7 (LOD 30, 127–140 Mb; MGSCv37 mm9) for both number and diameter (*Canq1*, here renamed *Candq1*).²² *Candq1* accounted for the majority of the variance, whereas weaker QTLs were also found for collateral number on chromosomes 1, 3 and 8.²² SNP-mapping of *Candq1* among the 21 strains using the Efficient Mixed Model Algorithm

(EMMA)²³ suggested a much narrower locus (132.36–132.82 Mb) and a 9-member candidate gene list.¹⁹ *Candq1* was also linked to variation in collateral remodeling through its linkage to variation in native collateral diameter^{18,22}—which is well-known to be the major determinant of the strength of the shear-stress stimulus that drives collateral remodeling.³

Interestingly, *Candq1* is identical in peak marker location to QTLs found earlier in B6 and Bc mice for recovery of hindlimb perfusion and tissue necrosis 21 days after femoral artery ligation (FAL) (*Lsq-1*)²⁴ and for infarct volume 24 hours after permanent MCAO (*Civq1*).²⁵ Based on haplotype analysis of *Lsq-1*, a list of 37 potential candidate genes was obtained,²⁴ while a refined haplotype analysis of *Civq1* gave a partially overlapping list of 12 candidates.²⁵ Neither list overlapped with the candidate genes derived from EMMA mapping for collateral number and diameter.¹⁹ Moreover, the distribution of infarct volumes across 15 strains²⁵ was closely predicted by the strain-specific values for collateral number, diameter, and length, plus hematocrit and MCA tree territory.¹⁸ Similarly, values for blood flow, hindlimb use and ischemic appearance immediately after and 21 days after FAL of B6, Bc and an F1 cross correlated with the high (B6), low (Bc), and intermediate (F1) number of collaterals in the adductor thigh region and cerebral cortex of these strains.²¹ This suggests that genetic variation in native collateral extent is the major physiological substrate responsible for the variation in blood flow and tissue injury in brain and hindlimb following arterial obstruction and for the three coincident QTLs on chromosome 7.^{19,22}

Taken together, the above studies present a significant conundrum. They propose 3 different candidate gene lists for a single phenomenon. Although there is strong evidence^{18–22} that variation in the extent of the native collateral circulation is a major factor underlying variation in the above ischemic injury traits—including the conclusion that *Candq1* and *Civq1* may be one and the same^{18–22,26}—differential metabolic sensitivity of cells to hypoxia/ischemia has recently been proposed to be a significant determinant of the variation in response to ischemia conferred by *Candq1* and *Lsq-1*.²⁶ This hypothesis would suggest that the three coincident QTL cover multiple processes, the loci for which would presumably cease to overlap with dissection of *Candq1* into smaller regions. To address the above uncertainties, we constructed a series of congenic mouse strains in which sub-regions of *Candq1* from B6 were introgressed into the Bc genome, and used them to examine 3 aims: 1) To establish the most cogent gene list possible to guide future investigation. 2) To determine whether collateral extent, infarct volume following MCAO, and perfusion and tissue injury following FAL continue to segregate together as the introgressed region becomes smaller. Such a finding would strengthen the hypothesis that genetic-dependent variation in collateral extent underlies the above QTL and is the major physiological factor responsible for the differences in ischemic tissue injury in B6, Bc and related mouse strains. 3) To generate a congenic strain-set with wide differences in collateral extent for use in future investigations of the collateral circulation.

METHODS

See online Data Supplement at <http://circres.ahajournals.org> for details.

Animals

Congenic strains were prepared by backcrossing B6-x-Bc recombinant inbred strains CXB3 and CXB4²⁷ to Bc, then successively backcrossing the progeny to Bc (~1500 mice bred and genotyped). *Cln3*^{Δex7/8} mice²⁸ and *Cln3*^{LacZ/LacZ} (Δ ex1–8)²⁹ (on B6 backgrounds) were from Jackson Laboratories and Dr. Beverly Davidson, respectively. Mice engineered with floxed alleles or made globally hypomorphic at *Jmjd5* (*Jmjd5*^{Neo/+}) (B6 background) were from Dr. Takeshi Suzuki.³⁰ Floxed mice were bred with B6-Cre mice to produce mice null

for *Jmjd5* in endothelial cells (*Jmjd5^{ECΔ}*) or globally haploinsufficient (*Jmjd5^{Δ/+}*). Gender does not influence collateral extent in brain or hindlimb,^{18,21} thus cohorts were ~half male and half female, and 2–4 mos-age. Approximately 2000 mice were bred, genotyped, and phenotyped for this study.

Collateral number, diameter and remodeling

The vasculature was maximally dilated and filled with Microfil™ with viscosity adjusted to minimize entrance into capillaries, followed by fixation and digital morphometry to obtain baseline collateral number and diameter and collateral remodeling 3 days after MCAO.¹⁶ Since collaterals of the neocortex in mouse (and human) reside in the *pia mater* with none in the brain parenchyma,^{31,32} their extent can be fully quantified using these methods.

Cerebral infarct volume

The right MCA trunk below the mid-temporalis muscle was permanently occluded (MCAO).¹⁶ Brain slices were stained with 2,3,5-triphenyltetrazolium chloride (TTC) 24 hours later.

Cerebral blood flow

In separate mice, the vasculature was maximally dilated and PBS containing 6-micron fluorescent microspheres and vasodilators was perfused retrograde via the thoracic aorta 24 hours after MCAO, followed by TTC staining of brain slices. Relative blood flow was quantified as the number of trapped microspheres in the volume of infarcted brain, normalized to the number trapped in the corresponding region/volume on the non-ligated side.^{33–35}

Hindlimb ischemia

Femoral artery ligation (FAL), laser Doppler measurement of plantar perfusion, which correlates closely with overall hindlimb blood flow,³⁶ and measurement of hindlimb use and ischemic appearance were as described.^{20,21}

Websites

See Online Table I for websites of databases used.

Statistics

Values are mean±SE. Data were tested with *t*-tests or ANOVA followed by Bonferroni *post-hoc* tests (significance at $p<0.05$).

RESULTS

Construction of congenic strains

Congenic (CNG) strains were derived from two B6×Bc (CXB) inbred lines in which homozygous blocks of B6 and Bc genotype are arranged in patchworks unique to each line.²⁷ CXB3 and CXB4 were chosen because they contained potentially advantageous breakpoints within *Candq1* near the EMMA region (Figure 1A). Congenic strains were developed by repeated backcrossing of CXB3 and CXB4 mice and progeny to Bc. At each round, congenic development was accelerated by screening progeny for loss of B6 genotype outside of *Candq1*. This resulted in 6 CNG strains, in 5 of which the introgressed B6 genotype successively converges on the center of the 95% confidence interval of *Candq1* (Figure 1A). In the exception, CNG1, the block of B6 ends at least 1 Mb centromeric to

EMMA (Figure 1A). Strains CNG1, 2 and 6 were derived from CXB3; CNG3, 4, and 5 from CXB4.

Since the CXB input lines are 55–60% Bc and we selected against B6 outside of *Candq1* (see Online Methods), we began data collection at N5. To confirm that these mice were essentially congenic, two N5 mice each from CNG5 and CNG6 were subjected to whole-genome analysis using the megaMUGA chip (21,200 informative markers for B6 and Bcl; FP de Villena, unpublished). Small blocks of B6 genome outside *Candq1* were variously found on chromosomes 5, 8, 11 and 14, but the percentages of B6 alleles among the markers, most of them heterozygous, were <0.1%, 0.3%, 0.7%, and 2.1%, respectively. The phenotyping results that were obtained with N5 and N6 mice (Figure 1C, discussed below) were not different from preliminary phenotyping of N4 mice, confirming that this small degree of “contamination” is without effect on collateral extent. Subsequently, in 3 N8 CNG5-B6/Bc mice, B6 alleles were found at only 19, 34 and 34 SNPs of the 21,213 informative SNPs outside *Dce1*.

Collateral number and diameter co-segregate and identify a single 737 kb locus responsible for the large variability in collateral extent between B6 and Bc mice

The collateral traits—number and diameter—for wildtype Bc, CNG1-B6/B6 and CNGx-Bc/Bc mice ($x=2-6$) were comparable (~1.0 collateral ~12 μ m in diameter; Figure 1C). Thus, other genetic elements outside of *Candq1* that contribute to the more numerous and larger diameter collaterals that are present in wildtype B6 mice²² were eliminated from the congenics by generation N5. CNG1 mice were not studied further.

The heterozygous (CNGx-B6/Bc) and homozygous (CNGx-B6/B6) genotypes conferred a remarkably consistent allele-dose-dependent increase in collateral number and diameter onto the Bc genome that is indistinguishable among the groups ($P>0.7$) (Figure 1C). The amount of “rescue” of collateral number and diameter in CNG2–6 B6/B6 mice averaged $73\pm 1\%$ and $93\pm 6\%$, respectively ($83\pm 4\%$ for extent), of the wildtype B6 values. The residual differences in collateral number between CNG3/5 B6/B6 and wildtype B6 presumably reflect the impact of the 3 other small-effects QTL identified for collateral number in B6-x-Bc F2 mice.²² By contrast, *Candq1* was the only QTL identified for diameter in that study, which is consistent with the greater rescue of diameter in the congenics. Importantly, both phenotypic traits among CNG2–6 remained the same as the introgressed regions converged on the overlap zone of CNG5 and CNG6, 133.229 – 133.966 Mb. Furthermore, they ceased to include the EMMA region^{19,22} (Figure 1A; shown in detail in Online Figure I), indicating that this region (present in CNG2–4 but not in CNG5 and 6) has no detectable effect. These data suggest that the zone of overlap (0.737 Mb) contains the entire causal element of the originally defined²² 27 Mb QTL, *Candq1*, for both number and diameter. We designate this region as Determinant of collateral extent 1 (*Dce1*, detailed map in Online Figure IB).

Differences in collateral extent specified by *Dce1* account for the differences in severity of tissue injury in mouse models of ischemic stroke and peripheral artery disease

Given their ~isogenic background outside of *Dce1*, the above congenic strains provide a unique opportunity to determine the impact of differences in collateral extent, alone, on tissue injury after arterial occlusion, free of the many other genetic-dependent hemodynamic and molecular differences in B6 and Bc that could also cause differences in severity of ischemic tissue injury. In CNG3, CNG4, and CNG5 Bc/Bc mice, whose collateral extents do not differ from wildtype Bc (Figure 1C), infarct volume at 24 hours was not different from wildtype Bc (Figure 2). By comparison, in CNG3, CNG4, and CNG5 B6/B6 mice, whose collateral extents are rescued by 76, 91, and 82% (Figure 1C), infarct volume was dramatically returned toward the low value of wildtype B6 (rescue of 85%). Furthermore,

like collateral extent (Figure 1), rescue of infarct volume was intermediate in the heterozygote condition. This congruency strongly strengthens the conclusion that the difference in pial collateral extent is the major factor that determines the large difference in infarct volume between Bc and B6 mice, and by inference, among 15 inbred mouse strains examined previously.²⁵ As with collateral number, the small residual difference in infarct volumes between CNG3–5 B6/B6 and wildtype B6 may reflect the impact of the 3 other small-effects QTL identified for collateral number in B6-x-Bc F2 mice.²²

To test the hypothesis that the protective mechanism provided by the B6 allele of *Dce1* is collateral-dependent blood flow, we measured flow in the infarct zone of CNG4-B6/B6 and CNG4-Bc/Bc 24 hours after MCAO using the microsphere method.^{33–35} Baseline blood flow (non-ligated side) did not differ between strains (data not shown). Flow in the infarcted region was 4.5-fold higher in B6/B6 mice (or 73% lower in Bc/Bc) (Figure 3). The higher flow reduced but did not prevent some infarction. The latter is expected, given that significant oxygen already diffuses from the ACA and PCA trees before traversing the collaterals, and given that the estimated relative conductance of the native pial collateral network in aggregate (including PCA↔MCA collaterals that typically number ~5 per hemisphere in wildtype B6 mice and are larger in diameter) is 15–20 % of the conductance of the trunk of the MCA tree at the site of ligation in wildtype Bc (Faber et al, unpublished).

We have shown that genetic strain-specific differences in collateral extent in brain are shared in other tissues of the same mouse strains, including skeletal muscle.^{20,21} To determine whether this extends to the *Dce1* allele, we also examined skeletal muscle. Unlike pial collaterals that can be measured with high fidelity, quantification of native collaterals in the hindlimb that mostly reside deep in the adductor thigh where they cross-connect arterial trees that branch in 3-dimensions, relies on the limited resolution of x-ray angiography^{20,21} or optical clearance of tissue followed by manual dissection.¹⁷ Therefore, we examined collaterals in the sheet-like abdominal wall musculature of the mouse where, like in the pia, the vascular trees are arranged in 2-dimensions. In agreement with the above findings in brain, collateral number in CNG4-Bc/Bc did not differ from wildtype Bc, whereas the B6/B6 alleles of *Dce1* rescued collateral number to 54% of the 6-fold greater number in wildtype B6 (Figure 4).

We next examined a model of PAD to test the hypothesis that the above finding extends to the hindlimb and has functional significance. In support of this, blood flow determined immediately after FAL and use and ischemic appearance scores measured one day later in CNG4-Bc/Bc and CNG4-B6/B6 mice—values that are predominantly determined by native collateral extent in the thigh—closely mimicked those previously reported in the wildtype strains (Figure 5).^{20,21} That is, the B6/B6 allele of *Dce1* strongly rescued blood flow (perfusion was 73% greater than in CNG4-Bc/Bc immediately after FAL) and reduced/rescued the severity of hindlimb ischemia and use impairment on day-1 (88 and 100% reduction, respectively) (Figure 5C).

The improvement of blood flow that occurs over days-to-weeks after arterial occlusion primarily reflects anatomic lumen enlargement of collaterals, a process distinct from the process of collaterogenesis that occurs in the embryo/neonate.^{31,37} The latter, which is governed largely by *Candq1* in Bc and B6 mice, determines native collateral extent in the adult and sets the baseline diameter upon which remodeling operates.^{21,31} We previously found that *Candq1* had no effect on variation in collateral remodeling in B6 and Bc mice, apart from its effect on baseline collateral diameter and thus the shear stress stimulus that drives collateral remodeling after arterial occlusion.^{18,22} Consistent with this, the increase in hindlimb perfusion over day3–10 in CNG4-Bc/Bc was similar to wildtype Bc, while in CNG4-B6/B6 it was 83% greater than CNG4-Bc/Bc (Figure 5B) and was ~55% of wildtype

B6 (wildtype Bc and B6 values reported previously^{20,21}). Similar data were obtained for CNG5-B6/B6 (Online Figure II). In agreement with the above data, remodeling of pial collaterals 3 days after MCAO was comparable in B6/B6 and Bc/Bc congenic mice to their wildtype strains (Online Figure II). These data confirm previous findings that *Candq1* (*Dce1*) does not link to the component of genetic-dependent variation in remodeling that is independent of baseline diameter; a QTL for the latter was identified on chromosome 11.²²

Genetic analysis of Dce1

We next analyzed *Dce1* by evaluating published information available for the genes, single nucleotide polymorphisms (SNPs), haplotypes, other genetic elements within *Dce1*, and by evaluating knockout mice.

Gene analysis

Dce1 contains 28 protein-coding genes (Figure 1A and Online Table II). In contrast to the previous candidate lists for *Candq1* and coincident QTLs (see Introduction), in which no gene had clear ties to vascular biology,^{19,24,25} seven genes in *Dce1* can be at least provisionally tied to endothelial cell (EC) biology (*Rabep2*, *Sh2b1*, *Cln3*, *Apobr*, *Il27*, *MapK3*, and *Ppp4c*; Figure 6) (discussed below). We focused on ECs because collateralogenesis occurs in the embryo by EC sprouting that involves VEGF-A, Flk1 (VEGFR2), Clic4 and Notch signaling,^{37,38,39} because collateral extent is altered in adult mice with altered expression of eNOS,³⁷ Dll4,⁴⁰ connexin 40^{41,42} and synectin,⁴³ and because all of these genes are strongly expressed in ECs.

Two *Dce1* genes listed above contain non-synonymous SNPs. The substitutions R298Q in *Rabep2* and H120Y in *Cln3* are predicted to be “probably damaging” for protein function (PolyPhen-2; scores > 0.999–1.0). Both proteins are intriguing since they are involved in intracellular membrane trafficking, which is central to VEGF signaling.^{44–46} Ligated VEGFR2 becomes phosphorylated and is internalized in complex with NRP-1 to early endosomes under the control of Rab5. It then moves to Rab4 vesicles, the fast recycling pathway, and then to Rab11, the slow recycling pathway. While internalized, the kinase domain of VEGFR2 continues to signal downstream, notably to MapK3 (ERK1/2, p44/42),⁴⁷ and entry into the slow recycling pathway alters signaling.⁴⁴ *Rabep2* (Rabaptin-5beta) is a homolog of *Rabep1* (Rabaptin-5), which in complex with *Rabgef1* (Rabex-5) is an effector protein for Rab5 in the control of fusion of endocytic vesicles to form the early endosome and for Rab4 in subsequent control of rapid endocytic recycling.^{45,48} *Rabep2* binds Rab5, Rab4 and *Rabgef1*, co-localizes with Rab5 on endosomal membranes, and is necessary for full endosome fusion activity *in vitro*.^{45,48,49} The amino acids at position 298 in *Rabep2* and the corresponding position (K578) in *Rabep1* are conserved among *Rabep* sequences. Replacement of K578 in *Rabep1* by glutamine is predicted to be only “possibly damaging” (score 0.694 by PolyPhen-2), but there are no relevant experimental data on *Rabep1* or 2. Interestingly, *Rabep2* contains the highest density of SNPs in *Dce1* (Figure 6C, see below). We are currently generating mice with disruption of *Rabep2* since they have not been described.

Cln3, the gene responsible for juvenile Batten’s disease, codes an intracellular transmembrane protein believed to be involved in late endosomal trafficking and lysosome function.^{50–53} In mouse brain, *Cln3* is expressed almost exclusively in ECs during the time of collateralgenesis (embryonic days E14.5–E18.5³⁷).²⁹ We thus examined two different *Cln3*^{-/-} mice^{28,29} but observed no effect on collateral extent (Online Figure III).

The only other non-synonymous SNP in *Dce1* is in the T-box transcription factor, *Tbx6*,⁵⁴ giving the substitution Q331R, which is predicted to have no effect on protein function by

Polyphen-2. This SNP and 3 others in *Tbx6* also occur in one or more strains with high collateral extent (CAST/EiJ, NOD/ShiLtJ),¹⁹ suggesting that *Tbx6* is an unlikely candidate gene (see SNP analysis, below). However, in a previous study, we determined relative expression levels of 106 genes, including all 28 in *Dce1*, in the *pia mater* dissected from brains of B6 and Bc embryos at 3 time-points spanning the time of collateralogenesis.¹⁹ Differential expression of *Tbx6*, *Nfatc2ip* and *Slx1b* achieved significance (Bc>B6) with *Tbx6* being the most strongly upregulated (2.9-fold). There are no reports of *Tbx6* expression in ECs cells or interaction with VEGF. However, *Tbx6* has been shown to cooperate with Notch intracellular domain in controlling expression of *Hes7* and *Mesp2*.^{55–57} Thus, *Tbx6* could be involved in vessel patterning⁵⁸ and/or collateralogenesis.³⁷ We are currently generating mice with disruption of *Tbx6* since they have not been described.

Nfatc2ip (*Nip45*) is a modulator of the type 2 T helper cell immune response in mice, with the type 2 response being characteristic of Bc but not B6 mice. *Nfatc2ip* has a candidate SNP in its 3'UTR (see below), which could explain the differential pial expression, although *Nfatc2ip* mRNA is not recognized as an experimentally supported miRNA target (TARbase v. 6.0).⁵⁹ *Slx1b* is annotated as SLX1 structure-specific endonuclease subunit homolog B. There are no reports of either *Nfatc2ip* or *Slx1b* in ECs. We are currently generating mice with disruption of these genes, since they have not been described.

Jmjd5 (lysine-specific demethylase 8) was a particularly intriguing gene in the EMMA region because of possible roles in transcriptional and epigenetic regulation, and a strong argument was made for it as a candidate gene for *Candq1*.¹⁹ However, collateral extent in mice globally haploinsufficient, globally hypomorphic, or with EC-specific knockout of in *Jmjd5* were not different from wildtype littermates (Online Figure IV).

Evidence that *Sh2b1*, *Apobr*, *Il27*, and *Ppp4c* are potential candidate genes is summarized in the Online Supplement.

Dce1 is partially syntenic with human 16p11.2, a locus strongly implicated in neurodegenerative disease, schizophrenia, autism, and severe early onset obesity.^{60–62} However, we found no reports of vascular disease associated with 16p11.2 or hits in GWAS studies in 16p11 for vascular deficiencies.

SNP analysis

SNPs in *Dce1* (Mouse Phenome database, Mouse Genomes Project) were evaluated in the LookSeq pileups of deep sequencing data for Bc and B6 (see URLs in Online Table I). This gave 72 high confidence SNPs. In a parsimonious model, a SNP responsible for low collateral extent would be present in Bc and AKR/J, a low-collateral strain (averaging 4.8 pial collaterals)¹⁸ that is phylogenetically identical to Bc in *Dce1*, but would not be present in high collateral strains. Accordingly, we examined each SNP location in the high collateral strains for which LookSeq data are available (LP/J, C3H/HeJ, CAST/EiJ, CBA/J, DBA/2J, FVB/NJ, NOD/ShiLtJ, and 129S1/SvimJ, plus A/J, a moderately low collateral strain (7 collaterals)^{18,19} This yielded 27 candidate SNPs (Online Table III) present in Bc and AKR but not in the high collateral strains.

Five additional strains support the above SNP identifications. C57BLKS/J, 129X1/SvJ, and KK/HiJ, are high collateral strains that have the B6 allele at each candidate SNP. SWR, the strain having the lowest number of collaterals after Bc (2.6 collaterals),¹⁸ is phylogenetically identical to Bc in *Dce1* and has the Bc allele at each candidate SNP. On the other hand, SJL (high, at 19.2 collaterals) and NZW (medium, at 8.3) are also identical to Bc in *Dce1*. The strong influence of *Dce1* for determination of collateral extent can apparently be overridden by loci elsewhere in the genome. These may include the loci on chromosomes 1, 3 and 8

identified in B6-x-Bc F2 crosses,²² but a SJL-x-SWR-F2 failed to find any significant QTL.¹⁹ Recently, Chu et al⁶³ applied a similar strategy to B6 and C3H/HeJ, which are similar in collateral number but different in collateral diameter¹⁸ and cerebral infarct volume,²⁵ and identified a locus linked to infarct volume on chromosome 8 (*Civq4*) that is coincident with *Canq4*.²² Mapping of number and diameter did not identify a significant QTL on chromosome 8 in this cross (however, 50% fewer F2 mice were phenotyped for collateral traits and those traits had 5-fold smaller ranges than infarct volume). The authors concluded that *Civq4* affects infarct volume in a collateral-independent manner.⁵³ Such a finding could have important ramifications. However, the conclusion remains uncertain because, compared to B6 mice, C3H/HeJ have smaller collateral diameters, trend smaller in number,^{18,63} and have lower blood pressure⁶⁴ and hemoglobin content than B6.⁶⁵ Mouse Phenome Database These differences are relevant because oxygen delivery across a collateral network after occlusion is proportional to [collateral number \times diameter⁴ \times arterial pressure \times arterial oxygen content]. Thus, even a “small” reduction in collateral extent in the C3H/HeJ strain would result in a significantly greater infarct volume after MCAO.

Haplotype analysis

The genomes of the classical inbred mouse strains are assemblies of a blocks of DNA (haplotypes) identical by descent from ancestral populations and recognizable by their numbers and distributions of SNPs.⁶⁶ Therefore, an alternative model is that the causal element(s) in *Dce1* lies in a haplotype, possibly enclosing collateral-influencing elements that are linked or have interacting effects. *Dce1* contains 3 haplotype blocks between B6 and Bc (Figure 6A). These blocks contain 11 genes and 15 of the 27 candidate SNPs (Figure 6B). Of the 11 genes, only 2 (*Rabep2* and *Sh2b1*) can be linked through the literature to possible roles in vascular biology.

The genes identified for relevance to vascular biology, proximity to candidate SNPs, and location in Bc haplotype blocks are listed in Figure. 6B. The only gene present in all 3 lists is *Rabep2*, in haplotype block 2, which contains 14 of the 27 candidate SNPs, 7 of which are in *Rabep2* (Figure 6C). These analyses thus converge on haplotype block 2, and suggest *Rabep2* in particular, as a possible causal element in *Dce1*.

Other genetic elements in *Dce1*

No conventional miRNAs were found in *Dce1*, but miRBase lists 2 “5p-tailed mirtrons”, or miRNAs located in intronic sequences at splice junctions.⁶⁷ Nothing is known of their possible functions. NONCODE v.4 lists 51 long noncoding RNAs (2 exons, >200 base pairs), including 24 long intervening RNAs (ie, between coding genes) and 27 that overlap protein coding genes (reviewed in Ulitisky and Bartel).⁶⁸ None of these appear to be annotated regarding regulatory or small peptide coding functions or strain-differences in expression. The longest of these transcribes exons 3–11 of *Rabep2* and terminates at exons 14 and 15 of *Atp2a1* (transcribed from the opposite strand), adding to the intrigue of *Rabep2*. We also examined indels and structural and copy number variations in Bc versus B6 in the Mouse Phenome Database. All 60 indels (Sanger2 data set in the Mouse Phenome Database) were intergenic or intronic and usually located in highly repetitive sequences. Three structural variations were small (240, 225 and 3 bases, Sanger3 data set) and located intergenically or near the center of large introns. No copy number variations were listed (Amgen1 data set). None of these elements were studied further.

DISCUSSION

The possibility that variation in the extent of the native collateral circulation is an important determinant of variation in ischemic injury when acute arterial occlusion occurs or disease

becomes manifest, has historically been overlooked or minimized—with the exception of those who study or treat acute ischemic stroke, eg, 7–14 and refs therein some coronary investigators, eg, 4–6,69 and refs therein and among vascular surgeons who frequently encounter or perform arterial occlusions.^{70,71} This presumably extends, in part, from the small diameter typical of native collaterals in most healthy individuals that is beyond the resolution of digital angiography (>0.2 mm), the misconception that such minute vessels cannot mediate significant flow in the acute setting until remodeling has occurred, and from the inability to experimentally change native collateral extent to test its importance. The latter restriction has begun to yield in recent studies where collateral extent was found to vary widely in mice with differences in genetic background.^{18–22,31,72} This variation was strongly correlated with differences in blood flow, tissue injury and functional impairment after acute occlusion and in chronic recovery of flow and function during collateral remodeling. However, whether these associations reflects a *causal* relationship could not be determined because it was not been possible to change native collateral extent while keeping genetic background constant. Even in inbred mice, including Bc and B6 strains, differences in genetic background have significant effects on arterial pressure, microvascular regulation, blood rheology, sensitivity of tissue to ischemia, immune response, inflammation, expression of a many vascular-acting genes, and additional mechanisms that can each affect collateral flow and tissue injury after acute and chronic arterial occlusion independent of differences in native collateral extent (eg, see Mouse Phenome Database and Discussion/ references in 18–22,26,31,38, 64).

In the present study, we addressed this uncertainty by generating a congenic set of (CNG5, currently backcrossed to effectively “N10”, see Results) with *Dce1* allele-dose-dependent differences in collateral extent that are essentially isogenic elsewhere in their genomes. We show that congenic introgression of the *Dce1* locus (737 Kb) of “high-collateral” B6 mice into the genome of “low-collateral” Bc mice confers near-B6 levels of native collateral number and diameter in the brain, as well as cerebral blood flow and infarct volume following MCAO. Furthermore, we obtained similar effects for native collaterals in skeletal muscle, as well as hindlimb blood flow, ischemic tissue appearance and use-impairment and recovery of these parameters immediately after and on subsequent days following FAL. This confirms previous studies^{20,21,38–40} showing that genetic effects on collateral extent apply to multiple tissues for a given genetic background. The magnitude of the residual trait-differences between congenic B6 strains and B6 wildtype mice agree with previous estimates of the effect-size of three additional minor QTL for collateral number and/or diameter.²² Thus, congenic substitution of a discrete locus strongly reduced the tissue injury in models of stroke and PAD that occurs in a strain with poor collateral extent. These findings demonstrate the importance of the native collateral circulation in determining the severity of ischemic injury and capacity to recover blood flow and tissue function after arterial occlusion. They also validate this same conclusion suggested in previous studies examining different mouse strains.^{18–22} Thus, at least in the healthy young adult strains examined thus far, genetic-dependent variation in native collateral extent strongly dominates the above-mentioned collateral-independent factors in determining tissue injury.

Congenic introgression of the B6 allele of *Dce1* into the Bc background rescued (“restored”) collateral number to 85% of wildtype B6 in brain, but only 55% in skeletal muscle (Figures 1 and 4). This difference may reflect that muscle types differ greatly in arterial branch-patterning and metabolic fiber type composition, ie, that the external and internal oblique muscles and rectus abdominus, which compose the abdominal area that we studied, may not be representative of all skeletal muscles viewed as a whole, with regard to collateral extent. As stated in Results, we phenotyped this muscle area because, unlike other muscles but much like the pial circulation, its arterial architecture is arranged in two dimensions and thus can be imaged with high fidelity. The above difference could also reflect differences in the

timing of collateralogenesis that may exist among different tissue types during development and tissue growth, or differences in contribution of *Dce1* to the extent of the native collateral circulation. Regarding the latter, 3 additional small-effect QTL for collateral number were identified in our earlier study.²² However, despite the difference in rescue shown herein, these findings confirm previous work showing the dominance of the chromosome 7 locus, now refined to *Dce1*, in determining the majority of the differences in collateral abundance in multiple tissues of the mouse.^{18–22}

Based on differential responses of skeletal muscle cells from B6 and Bc mice to hypoxia/ischemia *in vitro*, it was recently proposed that besides controlling collateralogenesis, *Candq1* also harbors a non-vascular, muscle cell-autonomous gene(s)—involved in plasticity and survival of muscle precursor cells and expression of vascular factors and their cognate receptors—that is important in the response to ischemia independent of differences in collateral extent.²⁶ This proposal, together with the fact that *Civq1* for infarct volume after MCAO is coincident with *Candq1* and *Lsq-1*, thus suggests that the three QTL cover multiple processes. If correct, the loci for these different processes should cease to overlap during congenic dissection of *Candq1*. This should result in a retention of the trait-values for (ie, rescue of) collateral extent and collateral-dependent perfusion, but a reduction in the rescue of cerebral infarct volume after MCAO and hindlimb ischemic injury and use after FAL, or a separation of the two processes in certain congenic strains. However, our findings that congenic strains successively narrowing *Candq1* from 27 Mb to 737 kb retain the same values for all of these traits as the original interval, do not support this proposal.²⁶ Notwithstanding the possibility that the above non-vascular process remains within this narrow locus,⁶³ the current findings strengthen the conclusion that *Candq1*, *Civq1* and *LSq-1* are QTLs for a single phenotype, collateral extent, and that the common causal element, ie, one of the genetic elements presented in Results and Figure 6, lies in *Dce1*.

Identification of *Dce1* adds a fourth list of candidate genes in the search for the genetic basis of variation in collateral extent. The EMMA analysis of 21 strains,¹⁹ which confirmed our F2 cross,¹⁸ came very close to pinpointing *Dce1*. It may have missed because of this limited number of strains⁷³ and possibly because of effects of strains A/J (very different from Bc at *Dce1* but with low collateral number) and SJL/J (identical to Bc at *Dce1* but with high collateral number). Similarly, the efforts to identify causal elements and candidate gene lists in *Civq1*²⁵ and *LSq-1*²⁴ were deflected from *Dce1* because they depended on the reasonable assumption that causal elements would be identical between A/J and Bc, and distinct from B6. This assumption was based on the findings that chromosome substitution strain 7, in which B6 chromosome 7 is replaced by A/J chromosome 7, nearly phenocopies A/J,^{21,22,24,25} However, the haplotype structure of A/J in *Dce1* is quite distinct from those of Bc and B6 (1513 and 1526 SNPs, respectively,^{Mouse Phenome Database}) and none of the candidate SNPs in Figure 6 is present in A/J. These findings, when combined with our previous observation that collateral number and diameter were reduced by ~75% in B6 mice whose chromosome 7 had been substituted with that of the A/J strain,^{21,22} suggest that a different locus or one that interacts with *Dce1* is present on chromosome 7 of A/J mice. An obvious model which would reconcile these results and *Dce1* would suppose an element on chromosome 7, outside of *Dce1* and identical in Bc and A/J, that favors high collateral number if “activated” by a “signal” from an element in *Dce1* having the B6 genotype. The sequences of neither Bc nor A/J would be capable of such activation.

In conclusion, the results of this study provide strong evidence that genetic-dependent variation in collateral extent underlies the three previously identified QTL, *Candrq1*, *Civq1* and *Lsq-1*, and is the major physiological factor responsible for differences in ischemic tissue injury in brain and hindlimb after arterial occlusion in B6, Bc and related¹⁹ mouse strains. Our findings have also greatly narrowed the locus, denoted *Dce1* (Determinant of

collateral extent-1, 737 kb) and provided a gene list, refined by *in silico* analysis and use of knockout mice, to guide future investigation. Although the causative genetic element(s) at *Dce1* has not yet been identified, we speculate it is a major “driver gene” or critical link in the pathway that governs collaterogenesis, a process that occurs late during gestation and determines collateral extent in the adult.³⁷ Since the pathways governing angiogenesis during development are highly conserved, polymorphisms of this same genetic element or a related one in the signaling pathway controlling collaterogenesis may be important in the wide variation in collateral status in humans,^{4–14} ie, may constitute a risk allele for collateral insufficiency in brain and other tissues. This hypothesis, which is currently under investigation in patients with acute ischemic stroke,⁷⁴ is aided by the large effect-size of *Dce1*^{22,25} and the fact that the locus is contiguous on human chromosome 16. Lastly, we have generated a congenic strain-set (CNG5) with wide “allele-dose-dependent” differences in collateral extent. Since these mice are isogenic elsewhere in the genome, they provide a unique strain-set for future investigations of the collateral circulation, including to model patients with poor, intermediate and good collateral status.

Supplementary Material

Refer to Web version on PubMed Central for supplementary material.

Acknowledgments

The authors are grateful to Dr Kun Gao for phenotyping *Cln3*^{-/-} Davidson mice, Drs Kirk Wilhelmsen, Fernando Pardo-Manuel de Villena and Tim Wiltshire for helpful discussion, Drs Darla Miller and Fernando Pardo-Manuel de Villena for megaMUGA genotyping, and Drs Beverly Davidson and Takeshi Suzuki for generous gifts of *Cln3*^{-/-} mice and *Jmjd5*-engineered mice, respectively.

SOURCES OF FUNDING

NIH-NHLBI-HL083633, -HL111073 and -NINDS-NS083633 (JEF).

Nonstandard Abbreviations and Acronyms

A/J	A/J strain of inbred mice
AKR	AKR/J strain of inbred mice
B6	C57Bl/6J strain of inbred mice
Bc	BALB/cByJ strain of inbred mice
<i>Candq1</i>	The first QTL identified for variation in <u>C</u> ollateral <u>a</u> rtery <u>n</u> umber and <u>d</u> iameter
CNG	Congenic
<i>Dce1</i>	The first congenic locus identified that <u>D</u> etermines variation in collateral extent
EMMA	Efficient mixed model association algorithm
FAL	Femoral artery ligation
MCAO	Middle cerebral artery occlusion
Mb/kb	Mega- and kilo-base pair DNA
QTL	Quantitative trait locus
SNP	Single nucleotide polymorphism

REFERENCES

1. World Health Organization. <http://who.int/mediacentre/factsheets/fs310/en/>
2. Faber, JE.; Dai, X.; Lucitti, J. Genetic and environmental mechanisms controlling formation and maintenance of the native collateral circulation. In: Deindl, E.; Schaper, W., editors. *Arteriogenesis – Molecular Regulation, Pathophysiology and Therapeutics*. Shaker Verlag; 2011. p. 1-22.
3. Schaper W. Collateral circulation: Past and present. *Basic Res Cardiol*. 2009; 104:5–21. [PubMed: 19101749]
4. Meier P, Gloekler S, Zbinden R, Beckh S, de Marchi SF, et al. Beneficial effect of recruitable collaterals: A 10-year follow-up study in patients with stable coronary artery disease undergoing quantitative collateral measurements. *Circulation*. 2007; 116:975–983. [PubMed: 17679611]
5. Meier P, Hemingway H, Lansky AJ, Knapp G, Pitt B, Seiler C. The impact of the coronary collateral circulation on mortality: a meta-analysis. *Eur Heart J*. 2012; 33:614–621. [PubMed: 21969521]
6. Traupe T, Ortmann J, Stoller M, Baumgartner I, de Marchi SF, Seiler C. Direct quantitative assessment of the peripheral artery collateral circulation in patients undergoing angiography. *Circulation*. 2013; 128:737–744. [PubMed: 23817577]
7. Christoforidis GA, Karakasis C, Mohammad Y, Caragine LP, Yang M, Slivka AP. Predictors of hemorrhage following intra-arterial thrombolysis for acute ischemic stroke: the role of pial collateral formation. *AJNR Am J Neuroradiol*. 2009; 30:165–170. [PubMed: 18768718]
8. Miteff F, Levi CR, Bateman GA, Spratt N, McElduff P, Parsons MW. The independent predictive utility of computed tomography angiographic collateral status in acute ischaemic stroke. *Brain*. 2009; 132:2231–2238. [PubMed: 19509116]
9. Maas MB, Lev MH, Ay H, Singhal AB, Greer DM, Smith WS, Harris GJ, Halpern E, Kemmling A, Koroshetz WJ, Furie KL. Collateral vessels on CT angiography predict outcome in acute ischemic stroke. *Stroke*. 2009; 40:3001–3005. [PubMed: 19590055]
10. Lima FO, Furie KL, Silva GS, Lev MH, Camargo EC, Singhal AB, Harris GJ, Halpern EF, Koroshetz WJ, Smith WS, Yoo AJ, Nogueira RG. The pattern of leptomeningeal collaterals on CT angiography is a strong predictor of long-term functional outcome in stroke patients with large vessel intracranial occlusion. *Stroke*. 2010; 41:2316–2322. [PubMed: 20829514]
11. Menon BK, Smith EE, Modi J, Patel SK, Bhatia R. Regional leptomeningeal score on CT angiography predicts clinical and imaging outcomes in patients with acute anterior circulation occlusions. *AJNR Am J Neuroradiol*. 2011; 32:1640–1645. [PubMed: 21799045]
12. Shuaib A, Butcher K, Mohammad AA, Saqqur M, Liebeskind DS. Collateral blood vessels in acute ischaemic stroke: a potential therapeutic target. *Lancet Neurol*. 2011; 10:909–921. [PubMed: 21939900]
13. Liebeskind DS. Recanalization and reperfusion in acute ischemic stroke. *Faculty 1000 Medicine Reports*. 2010 Sep.:1–4.
14. Pandey AS, Thompson BG, Gemmete JJ, Chaudhary N. Cerebral collateral circulation: integral to defining clinical outcome in acute cerebral ischemia. *World Neurosurg*. 2012; 77:240–242. [PubMed: 22501018]
15. Menon BK, Smith EE, Coutts SB, Welsh DG, Faber JE, Damani Z, Goyal M, Hill MD, Demchuk AM, Hee Cho K-H, Chang H-W, Hong J-H, Sohn SI. Leptomeningeal collaterals are associated with modifiable metabolic risk factors. *Ann Neurol*. 2013 [Epub ahead of print].
16. Faber JE, Zhang H, Lassance-Soares RM, Prabhakar P, Najafi AH, Burnett MS, Epstein SE. Aging causes collateral rarefaction and increased severity of ischemic injury in multiple tissues. *Arterioscler Thromb Vasc Biol*. 2011; 31:1748–1756. [PubMed: 21617137]
17. Dai X, Faber JE. eNOS deficiency causes collateral vessel rarefaction and impairs activation of a cell cycle gene network during arteriogenesis. *Circ Res*. 2010; 106:1870–1881. [PubMed: 20431061]
18. Zhang H, Prabhakar P, Sealock RW, Faber JE. Wide genetic variation in the native pial collateral circulation is a major determinant of variation in severity of stroke. *J Cerebral Blood Flow Metab*. 2010; 30:923–934.

19. Wang S, Zhang H, Wiltshire T, Sealock R, Faber JE. Genetic dissection of the *Canq1* locus governing variation in extent of the collateral circulation. *PLoS One*. 2012; 7:31910.
20. Chalothorn D, Clayton JA, Zhang H, Pomp D, Faber JE. Collateral density, remodeling and VEGF-A expression differ widely between mouse strains. *Physiol Genomics*. 2007; 30:179–191. [PubMed: 17426116]
21. Chalothorn D, Faber JE. Strain-dependent variation in native collateral function in mouse hindlimb. *Physiol Genomics*. 2010; 42:469–479. [PubMed: 20551146]
22. Wang S, Zhang H, Dai X, Sealock R, Faber JE. Genetic architecture underlying variation in extent and remodeling of the collateral circulation. *Circ Res*. 2010; 107:558–568. [PubMed: 20576932]
23. Kang HM, Zaitlen NA, Wade CM, Kirby A, Heckerman D, Daly MJ, Eskin E. Efficient control of population structure in model organism association mapping. *Genetics*. 2008; 178:1709–1723. [PubMed: 18385116]
24. Dokun AO, Keum S, Hazarika S, Li Y, Lamonte GM, Wheeler F, Marchuk DA, Annex BH. A quantitative trait locus (*lsq-1*) on mouse chromosome 7 is linked to the absence of tissue loss after surgical hindlimb ischemia. *Circulation*. 2008; 117:1207–1215. [PubMed: 18285563]
25. Keum S, Marchuk DA. A locus mapping to mouse chromosome 7 determines infarct volume in a mouse model of ischemic stroke. *Circ Cardiovasc Genet*. 2009; 2:591–598. [PubMed: 20031639]
26. McClung JM, McCord TJ, Keum S, Johnson S, Annex BH, Marchuk DA, Kontos CD. Skeletal muscle-specific genetic determinants contribute to the differential strain-dependent effects of hindlimb ischemia in mice. *Am J Pathol*. 2012; 180:2156–2169. [PubMed: 22445571]
27. Williams RW, Gu J, Qi S, Lu L. The genetic structure of recombinant inbred mice: High-resolution consensus maps for complex trait analysis. *Genome Biol*. 2001; 2 research0046-research0046.0018.
28. Cotman SL, Vrbanc V, Lebel LA, Lee RL, Johnson KA, Donahue LR, Teed AM, Antonellis K, Bronson RT, Lerner TJ, MacDonald ME. *Cln3(deltaex7/8)* knock-in mice with the common *jnl* mutation exhibit progressive neurologic disease that begins before birth. *Hum Mol Genet*. 2002; 11:2709–2721. [PubMed: 12374761]
29. Eliason SL, Stein CS, Mao Q, Tecedor L, Ding SL, Gaines DM, Davidson BL. A knock-in reporter model of Batten disease. *J Neurosci*. 2007; 27:9826–9834. [PubMed: 17855597]
30. Ishimura A, Minehata K, Terashima M, Kondoh G, Hara T, Suzuki T. *Jmjd5*, an *h3k36me2* histone demethylase, modulates embryonic cell proliferation through the regulation of *cdkn1a* expression. *Development*. 2012; 139:749–759. [PubMed: 22241836]
31. Chalothorn D, Faber JE. Formation and maturation of the murine native cerebral collateral circulation. *J Molec Cell Cardiol*. 2010; 49:251–259. [PubMed: 20346953]
32. Vander Eecken HM, Adams RD. The anatomy and functional significance of the meningeal arterial anastomoses of the human brain. *J Neuropathol Exp Neurol*. 1953; 12:132–57. [PubMed: 13053234]
33. Loftus CM, Greene GM, Detwiler KN, Baumbach GL, Heistad DD. Studies of collateral perfusion to canine middle cerebral artery territory. *Am J Physiol*. 1990; 259:H560–H566. [PubMed: 2386228]
34. Engelhorn T, Doerfler A, Forsting M, Heusch G, Schulz R. Does a relative perfusion measure predict cerebral infarct size? *AJNR Am J Neuroradiol*. 2005; 26:2218–23. [PubMed: 16219825]
35. Reading SA, Brayden JE. Central role of TRPM4 channels in cerebral blood flow regulation. *Stroke*. 2007; 38:2322–2328. [PubMed: 17585083]
36. Chalothorn D, Zhang H, Clayton JA, Thomas SA, Faber JE. Catecholamines augment collateral vessel growth and angiogenesis in hindlimb ischemia. *Am J Physiol Heart Circ Physiol*. 2005; 289:H947–H959. [PubMed: 15833801]
37. Lucitti JL, Mackey J, Morrison JC, Haigh JJ, Adams RH, Faber JE. Formation of the collateral circulation is regulated by vascular endothelial growth factor-A and A Disintegrin and Metalloprotease Family Members 10 and 17. *Circ Res*. 2012; 111:1539–1550. [PubMed: 22965144]
38. Clayton JA, Chalothorn D, Faber JE. Vascular endothelial growth factor-A specifies formation of native collaterals and regulates collateral growth in ischemia. *Circ Res*. 2008; 103:1027–1036. [PubMed: 18802023]

39. Chalothorn D, Zhang H, Smith JE, Edwards JC, Faber JE. Chloride intracellular channel-4 is a determinant of native collateral formation in skeletal muscle and brain. *Circ Res.* 2009; 105:89–98. [PubMed: 19478202]
40. Cristofaro B, Shi Y, Faria M, Suchting S, Leroyer AS, Trindade A, Duarte A, Zovein AC, Iruela-Arispe ML, Nih LR, Kubis N, Henrion D, Loufrani L, Todiras M, Schleifenbaum J, Gollasch M, Zhuang ZW, Simons M, Eichmann A, le Noble F. Dll4-Notch signaling determines the formation of native arterial collateral networks and arterial function in mouse ischemia models. *Development.* 2013; 140:1720–1729. [PubMed: 23533173]
41. Buschmann I, Pries A, Styp-Rekowska B, Hillmeister P, Loufrani L, Henrion D, Shi Y, Duelsner A, Hofer I, Gatzke N, Wang H, Lehmann K, Ulm L, Ritter Z, Hauff P, Hlushchuk R, Djonov V, van Veen T, le Noble F. Pulsatile shear and *gja5* modulate arterial identity and remodeling events during flow-driven arteriogenesis. *Development.* 2010; 137:2187–2196. [PubMed: 20530546]
42. Fang JS, Angelov SN, Simon AM, Burt JM. Cx40 is required for, cx37 limits, postischemic hindlimb perfusion, survival and recovery. *J Vasc Res.* 2012; 49:2–12. [PubMed: 21986401]
43. Moraes F, Paye J, Mac Gabhann F, Zhuang ZW, Zhang J, Lanahan A, Simons M. Endothelial cell-dependent regulation of arteriogenesis. *Circ Res.* 2013; 113:1076–1086. [PubMed: 23897694]
44. Ballmer-Hofer K, Andersson AE, Ratcliffe LE, Berger P. Neuropilin-1 promotes vegfr-2 trafficking through rab11 vesicles thereby specifying signal output. *Blood.* 2011; 118:816–826. [PubMed: 21586748]
45. Hutagalung AH, Novick PJ. Role of rab gtpases in membrane traffic and cell physiology. *Physiol Rev.* 2011; 91:119–149. [PubMed: 21248164]
46. Lanahan A, Zhang X, Fantin A, Zhuang Z, Rivera-Molina F, Speichinger K, Prahst C, Zhang J, Wang Y, Davis G, Toomre D, Ruhrberg C, Simons M. The neuropilin 1 cytoplasmic domain is required for vegf-a-dependent arteriogenesis. *Dev Cell.* 2013; 25:156–168. [PubMed: 23639442]
47. Lampugnani MG, Orsenigo F, Gagliani MC, Tacchetti C, Dejana E. Vascular endothelial cadherin controls vegfr-2 internalization and signaling from intracellular compartments. *J Cell Biol.* 2006; 174:593–604. [PubMed: 16893970]
48. Gournier H, Stenmark H, Rybin V, Lippe R, Zerial M. Two distinct effectors of the small gtpase rab5 cooperate in endocytic membrane fusion. *EMBO J.* 1998; 17:1930–1940. [PubMed: 9524116]
49. de Renzis S, Sonnichsen B, Zerial M. Divalent rab effectors regulate the sub-compartmental organization and sorting of early endosomes. *Nat Cell Biol.* 2002; 4:124–133. [PubMed: 11788822]
50. Uusi-Rauva K, Kyttala A, van der Kant R, Vesa J, Tanhuanpaa K, Neefjes J, Olkkonen VM, Jalanko A. Neuronal ceroid lipofuscinosis protein *cln3* interacts with motor proteins and modifies location of late endosomal compartments. *Cell Mol Life Sci.* 2012; 69:2075–2089. [PubMed: 22261744]
51. Liiro K, Yliannala K, Ahtiainen L, Maunu H, Jarvela I, Kyttala A, Jalanko A. Interconnections of *cln3*, *hook1* and rab proteins link batten disease to defects in the endocytic pathway. *Hum Mol Genet.* 2004; 13:3017–3027. [PubMed: 15471887]
52. Fossale E, Wolf P, Espinola JA, Lubicz-Nawrocka T, Teed AM, Gao H, Rigamonti D, Cattaneo E, MacDonald ME, Cotman SL. Membrane trafficking and mitochondrial abnormalities precede subunit c deposition in a cerebellar cell model of juvenile neuronal ceroid lipofuscinosis. *BMC Neurosci.* 2004; 5:57. [PubMed: 15588329]
53. Cotman SL, Staropoli JF. The juvenile batten disease protein, *cln3*, and its role in regulating anterograde and retrograde post-golgi trafficking. *Clin Lipidol.* 2012; 7:79–91. [PubMed: 22545070]
54. Chapman DL, Agulnik I, Hancock S, Silver LM, Papaioannou VE. *Tbx6*, a mouse t-box gene implicated in paraxial mesoderm formation at gastrulation. *Dev Biol.* 1996; 180:534–542. [PubMed: 8954725]
55. Yasuhiko Y, Haraguchi S, Kitajima S, Takahashi Y, Kanno J, Saga Y. *Tbx6*-mediated notch signaling controls somite-specific *mesp2* expression. *Proc Natl Acad Sci U S A.* 2006; 103:3651–3656. [PubMed: 16505380]

56. Niwa Y, Masamizu Y, Liu T, Nakayama R, Deng CX, Kageyama R. The initiation and propagation of *hes7* oscillation are cooperatively regulated by *fgf* and *notch* signaling in the somite segmentation clock. *Dev Cell*. 2007; 13:298–304. [PubMed: 17681139]
57. Gonzalez A, Manosalva I, Liu T, Kageyama R. Control of *hes7* expression by *tbx6*, the *wnt* pathway and the chemical *gsk3* inhibitor *licl* in the mouse segmentation clock. *PLoS One*. 2013; 8:e53323. [PubMed: 23326414]
58. Suchting S, Freitas C, le Noble F, Benedito R, Breant C, Duarte A, Eichmann A. The *notch* ligand *delta-like 4* negatively regulates endothelial tip cell formation and vessel branching. *Proc Natl Acad Sci U S A*. 2007; 104:3225–3230. [PubMed: 17296941]
59. Vergoulis T, Vlachos IS, Alexiou P, Georgakilas G, Maragkakis M, Reczko M, Gerangelos S, Koziris N, Dalamagas T, Hatzigeorgiou AG. Tarbase 6.0: Capturing the exponential growth of *mirna* targets with experimental support. *Nuc Acid Res*. 2012; 40:D222–D229.
60. Walters RG, Jacquemont S, Valsesia A, et al. *Nature*. 2010; 463:671–675. [PubMed: 20130649]
61. McCarthy SE, Makarov V, Kirov G, et al. *Nat Genet*. 2009; 41:1223–1227. [PubMed: 19855392]
62. Kumar RA, KaraMohamed S, Sudi J, Conrad DF, Brune C, Badner JA, Gilliam TC, Nowak NJ, Cook EH Jr, Dobyns WB, Christian SL. Recurrent 16p11.2 microdeletions in autism. *Hum Mol Genet*. 2008; 17:628–638. [PubMed: 18156158]
63. Chu PL, Keum S, Marchuk DA. A novel genetic locus modulates infarct volume independently of the extent of collateral circulation. *Physiol Genomics*. 2013; 45:751–763. [PubMed: 23800850]
64. Smolock EM, Ilyushkina IA, Ghazalpour A, Gerloff J, Murashev AN, Lusic AJ, Korshunov VA. Genetic locus on mouse chromosome 7 controls elevated heart rate. *Physiol Genomics*. 2012; 44:689–698. [PubMed: 22589454]
65. Ohkura N, Oishi K, Sekine Y, Atsumi G, Ishida N, Matsuda J, Horie S. Comparative study of circadian variation in numbers of peripheral blood cells among mouse strains: unique feature of C3H/HeN mice. *Biol Pharm Bull*. 2007; 30:1177–1180. [PubMed: 17541178]
66. Yang H, Wang JR, Didion JP, Buus RJ, Bell TA, Welsh CE, Bonhomme F, Yu AH, Nachman MW, Pialek J, Tucker P, Boursot P, McMillan L, Churchill GA, de Villena FP. Subspecific origin and haplotype diversity in the laboratory mouse. *Nat Genet*. 2011; 43:648–655. [PubMed: 21623374]
67. Ladewig E, Okamura K, Flynt AS, Westholm JO, Lai EC. Discovery of hundreds of mirtrons in mouse and human small rna data. *Genome Res*. 2012; 22:1634–1645. [PubMed: 22955976]
68. Ulitsky I, Bartel DP. LincRNAs: Genomics, evolution, and mechanisms. *Cell*. 2013; 154:26–46. [PubMed: 23827673]
69. van den Wijngaard JP, Schulten H, van Horssen P, Ter Wee RD, Siebes M, Post MJ, Spaan JA. Porcine coronary collateral formation in the absence of a pressure gradient remote of the ischemic border zone. *Am J Physiol Heart Circ Physiol*. 2011; 300:H1930–H1937. [PubMed: 21398599]
70. Sneider EB, Nowicki PT, Messina LM. Regenerative medicine in the treatment of peripheral arterial disease. *J Cell Biochem*. 2009; 108:753–761. [PubMed: 19711369]
71. Annex BH. Therapeutic angiogenesis for critical limb ischaemia. *Nat Rev Cardiol*. 2013; 10:387–396. [PubMed: 23670612]
72. Helisch A, Wagner S, Khan N, Drinane M, Wolfram S, Heil M, Ziegelhoeffer T, Brandt U, Pearlman JD, Swartz HM, Schaper W. Impact of mouse strain differences in innate hindlimb collateral vasculature. *Arterioscler Thromb Vasc Biol*. 2006; 26:520–526. [PubMed: 16397137]
73. Flint J, Eskin E. Genome-wide association studies in mice. *Nat Rev Genet*. 2012; 13:807–817. [PubMed: 23044826]
74. Lee, Y.; Menon, B.; Huang, D.; Wilhelmsen, K.; Powers, W.; Jovin, T.; Marshall, R.; Parsons, M.; Ribo, M.; Selim, M.; Sheth, K.; Al-Ali, F.; Shuaib, A.; Demchuk, A.; Liebeskind, D.; Faber, J. GENetic Determinants of Collateral Status in Stroke - The GENEDCSS Study; 20th International Stroke Conference; 2014. (abstract).

Novelty and Significance

What is Known?

- In most tissues, adjacent arterial trees are connected by a small number of arteriole-to-arteriole anastomoses termed collateral vessels that, in the event of occlusion of an artery supplying one of the trees (eg, in stroke, myocardial infarction or peripheral artery disease) can have a significant protective effect.
- Collateral-dependent blood flow varies widely among “healthy” humans, i.e., those without obstructive disease; however, the mechanisms responsible for this variation are unknown.
- The number and diameters of collaterals vary widely among strains of inbred mice, indicating that collateral extent is strongly influenced by genetic background; a quantitative trait locus (QTL) on chromosome 7 has been linked to the majority of this variation, but proof that this locus also causes the variation in tissue injury among the strains has not been obtained.

What New Information Does This Article Contribute?

- Congenic mice have been generated in which successively smaller regions of chromosome 7 of C57Bl/6J mice (B6; high collateral number and diameter) are introgressed into the BALB/cByJ strain (Bc; very low collateral number and diameter).
- The main genetic element determining variation in collateral extent in the cerebral pial and skeletal muscle circulations in these congenic strains has been localized to 737 kilobases (*Dce1*) on chromosome 7.
- Substitution of the B6 allele of *Dce1* for the Bc allele imparts to Bc mice high collateral extent and correspondingly greater tissue perfusion and protection in models of stroke and peripheral artery disease, proving that genetic variation in native collateral extent is the major determinant of variation in ischemic damage.

Although no studies have been done, understanding the genetic determinants of the extent of the native collateral circulation in humans could have significant impact in assessing risk for severe ischemic outcomes and suggesting life style alterations prior to ischemic events, assessing suitability and choice of recanalization treatment after an event, and stratifying patients by genetically assessed risk in clinical trials. Previous work in mice identified a major 27 Mb-wide QTL for variation in collateral extent on chromosome 7. Others identified apparently identical QTLs for infarct volume in a stroke model and tissue loss in a peripheral artery disease model. Efforts to identify the causal elements in the QTL(s) relied on indirect analyses and inference to identify several candidate genes, none of which are known angiogenic genes. The direct congenic approach used here has sharply localized the causal region (*Dce1*) and suggested new candidate genes, several of which are known to have vascular actions. The causal relationship between collateral extent and tissue response in the congenic strains strongly suggests that the three above QTLs all arise from a single phenomenon, collateral extent. This study provides a new basis for identifying collateral genes and, potentially, for assessing genetic influences on collateral extent in humans.

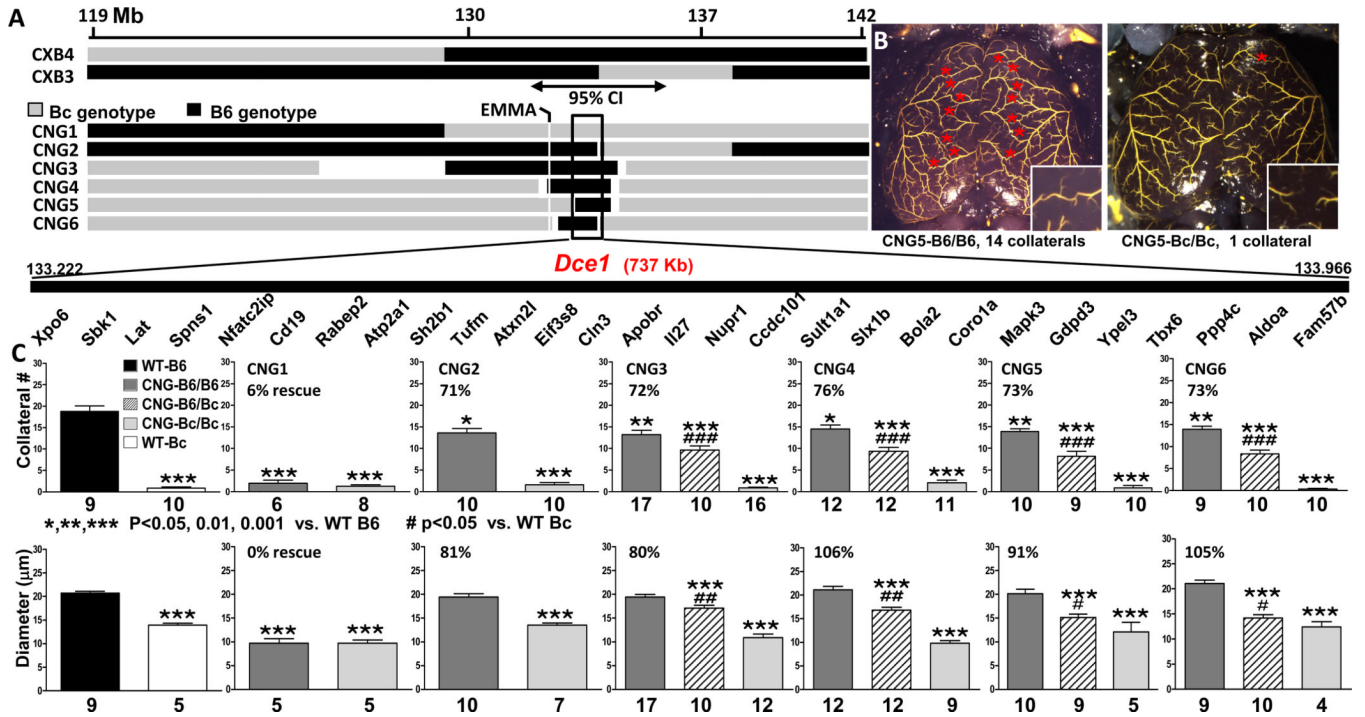
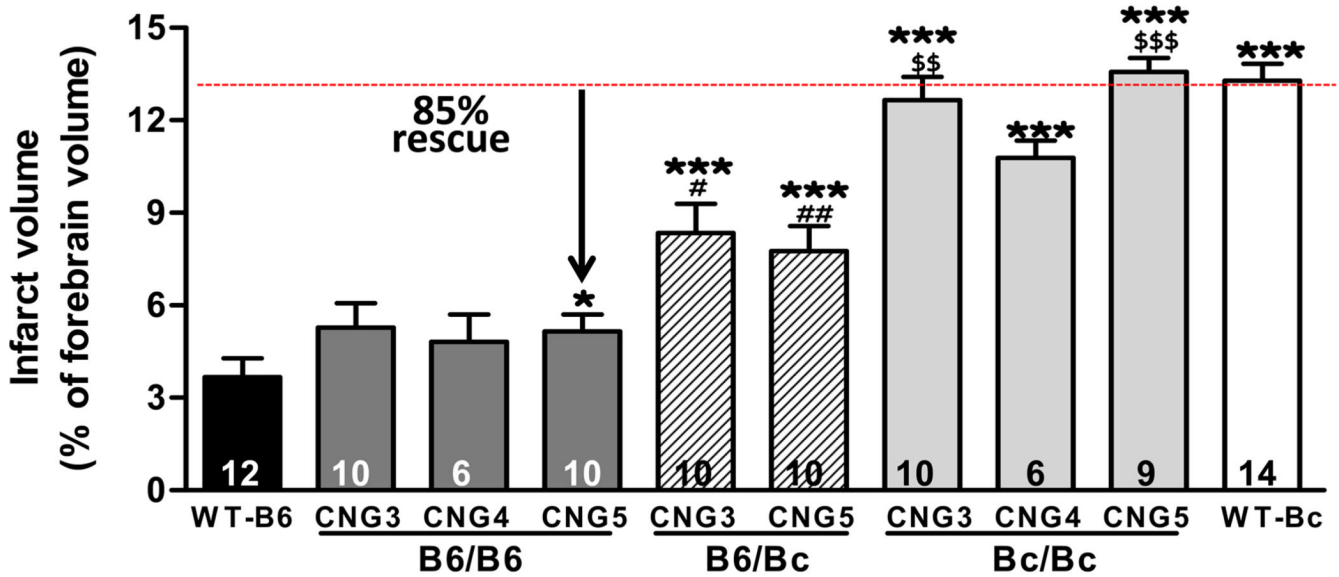
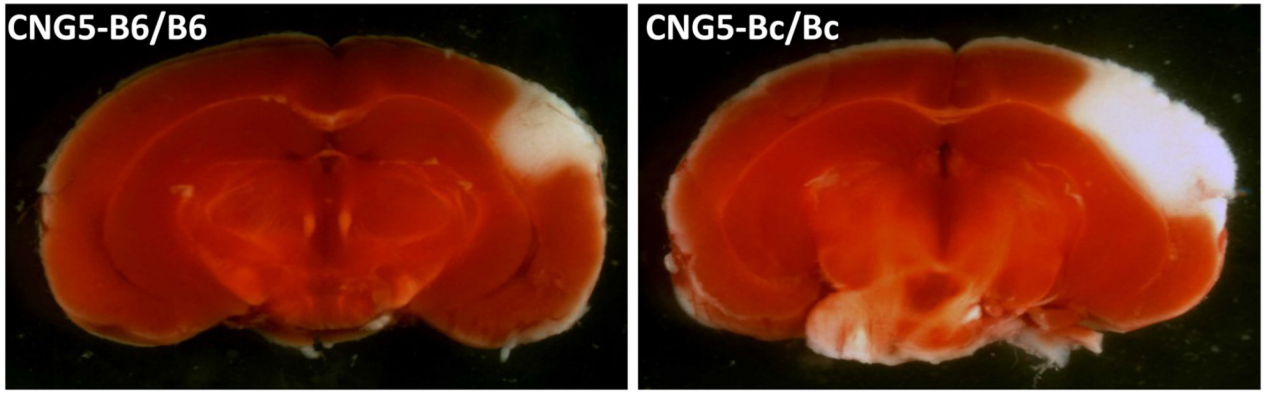


Figure 1. Introgression of *Dce1* into the Bc genome rescues collateral extent

A, Genetic maps of *Candq1*. **Upper**: input C57BL/6J × BALB/c recombinant inbred lines CXB3 and CXB4.²⁷ Black, genotype is B6; grey, Bc. Double-headed arrow: 95% confidence interval of *Candq1*.²² **Lower**: Congenic strains showing B6 regions introgressed into the Bc background. White indicates genotype uncertainty. The open rectangle indicates the zone of overlap (133.229 – 133.966 Mb; Build 37 mm9 coordinates) common to all but CNG1. The gene list in the overlap zone is not to scale. **B**, Filled pial pre-capillary vessels of 2–3 mos-old, maximally vasodilated CNG5 mice. Red stars: MCA-to-ACA collaterals. Insets: Collateral zones at higher magnification. **C**, Average MCA↔ACA collateral numbers (both hemispheres) and diameters in 2–3 mos-old wildtype B6 (black bar), wildtype Bc (white) and CNG mice. Charcoal, introgressed region is B6/B6; light grey, Bc/Bc; hatched, heterozygous. % rescue = (CNG-B6/B6 - wildtype B6) / wildtype B6 - wildtype Bc). Within each genotype (B6/B6, B6/Bc, and Bc/Bc), CNGs 2–6 were phenotypically indistinguishable in both number and diameter (ANOVA, 2-tailed), hence the causal element(s) for both lie in the overlap zone (*Dce1*, Determinant of collateral extent 1). CNG1 mice of all 3 genotypes had phenotypes like Bc and were not studied further. In all figures, numbers of mice are shown below or in each bar; for diameters in Bc/Bc mice, n's are low since many mice had no collaterals.



*, *** p<0.05, 0.01 vs. WT-B6 #, ## p<0.05, 0.01 vs. B6/B6 \$\$, \$\$\$ p<0.01, 0.001 vs. B6/Bc

Figure 2. Introgression of *Dce1* into the Bc genome rescues cerebral infarct volume

Cortical infarctions were produced in 2–3 mos-old CNG3, CNG5 and wild-type mice by permanent MCAO.^{16,18} 24 hours later, brains were sectioned (1mm) and TTC-stained to reveal non-viable tissue (white). Sections from the same brain level are shown. Infarct volumes expressed as % of total brain volume were determined from the complete set of sections in each brain. Within each genotype, CNG3, CNG4 and CNG5 are not significantly different even though the introgressed regions in CNG3 and CNG4 extend beyond that in CNG5 and include the EMMA peak (Figure 1A). This supports the conclusion that the causal element for infarct volume, as for pial collateral number and diameter, lies in *Dce1*. The B6/B6 genotype in CNG3, CNG4, and CNG5 rescues 85% of the difference between wildtype B6 and Bc.

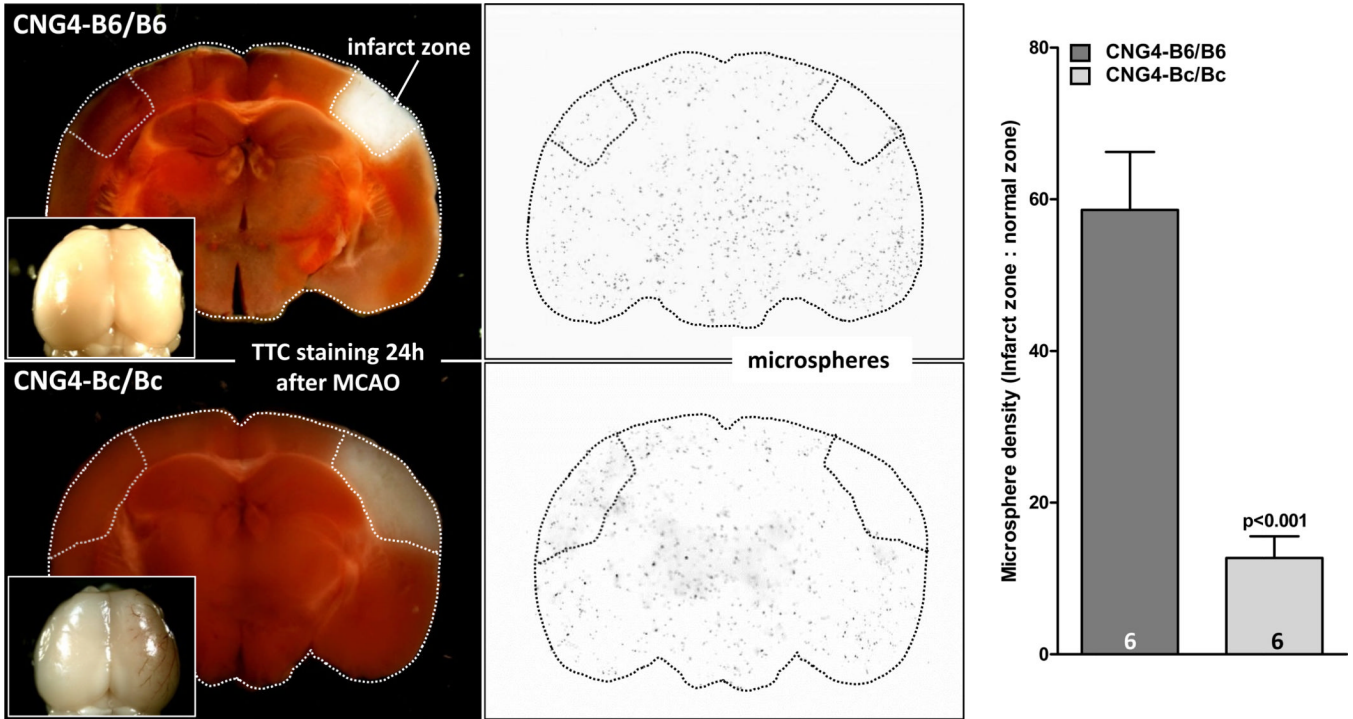


Figure 3. Introgression of *Dcel* into the *Bc* genome rescues blood flow after middle cerebral artery occlusion (MCAO)

24 hr after permanent MCAO, relative blood flow in the volume of infarcted brain and corresponding contralateral region (used for normalization) were determined using the microsphere method after maximal dilation. Relative blood flow was 4.5-fold greater in CNG4-B6/B6 compared to CNG4-Bc/Bc. Insets: Robust collateral-dependent retrograde perfusion in CNG4-B6/B6 is indicated by minimal brown clotted blood in the MCA territory, compared to the clearly visible brown tracks in the CNG-Bc/Bc brain. Baseline flow (non-ligated side) did not differ between strains.

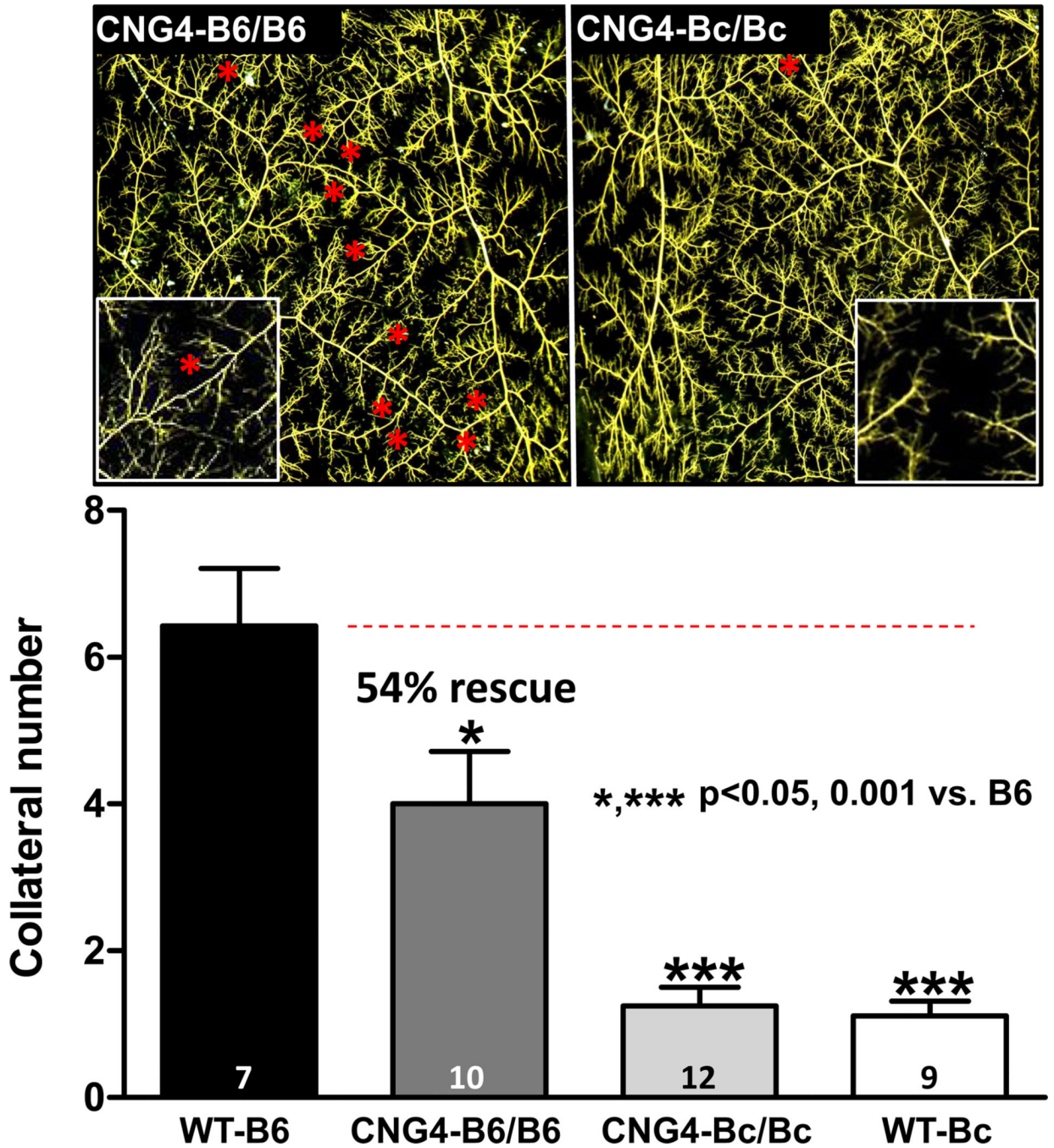


Figure 4. Introgression of *Dce1* into the Bc genome rescues collateral number in skeletal muscle
 Pre-capillary microcirculation in maximally dilated CNG4 and wildtype mice were filled with MicroFil. After fixation and optical clearing, collaterals between the epigastric and iliolumbar arteries, viewed from the peritoneal surface, were counted (red stars). Insets: collateral zones at higher magnification. The homozygous B6 *Dce1* allele restores 54% of the difference in collateral number between Bc and B6 wildtype mice.

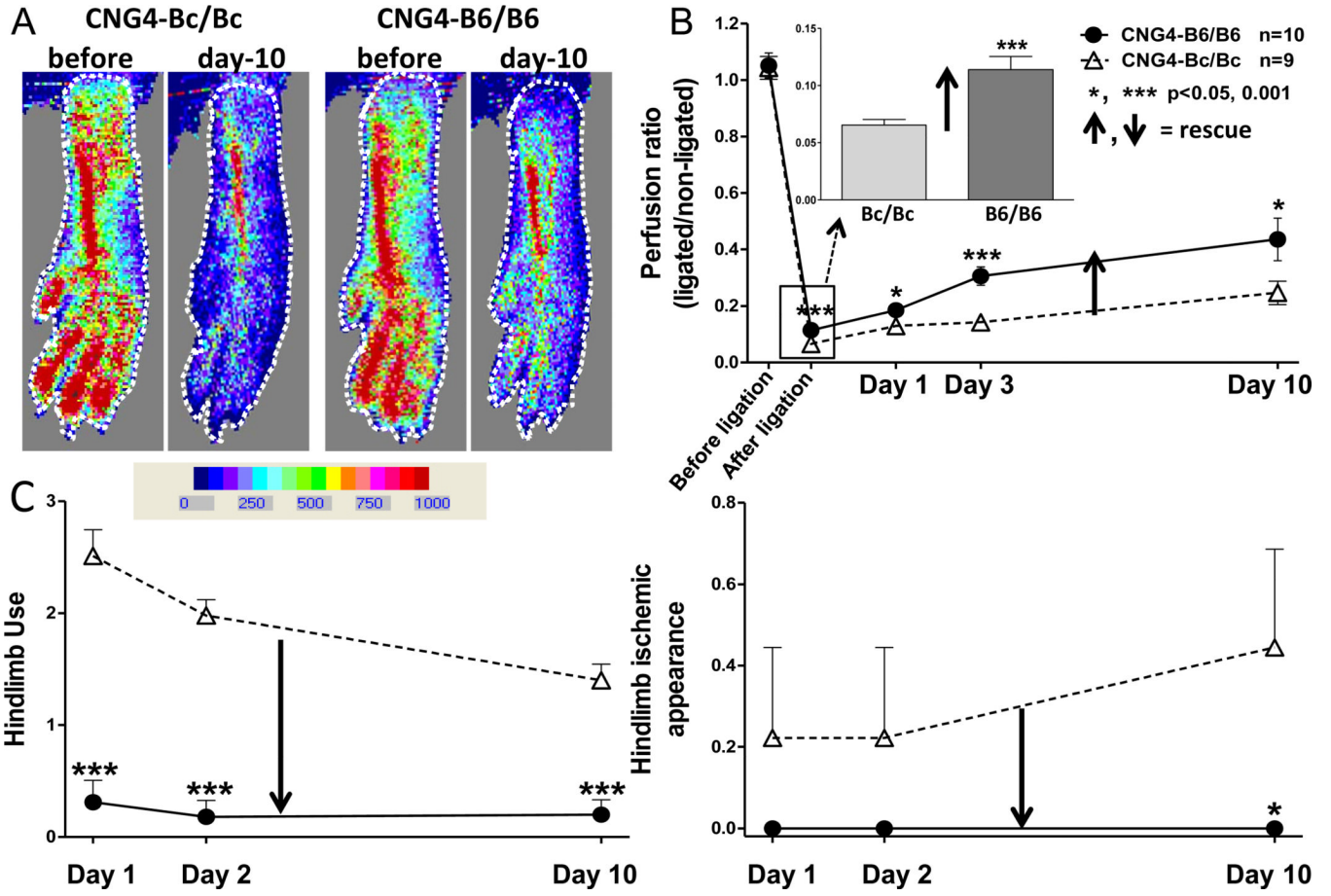


Figure 5. Introgression of *Dce1* into the *Bc* genome rescues hindlimb perfusion following femoral artery ligation (FAL)

A, Laser Doppler perfusion images of plantar region-of-interest (dotted line; quantified in panel B) before and after FAL. **B**, 73% greater perfusion immediately after FAL in B6/B6 is in agreement with greater native collateral extent in skeletal muscle (Figure 4); larger deviation at day-3 and day-10 is consistent with outward remodeling of a greater number of collaterals. Recovery of perfusion at day-10 was 83% greater in B6/B6. **C**, Severity of hindlimb use-impairment and ischemic appearance were reduced/rescued on day-1 by 88 and 100%, respectively, and were less severe thereafter.

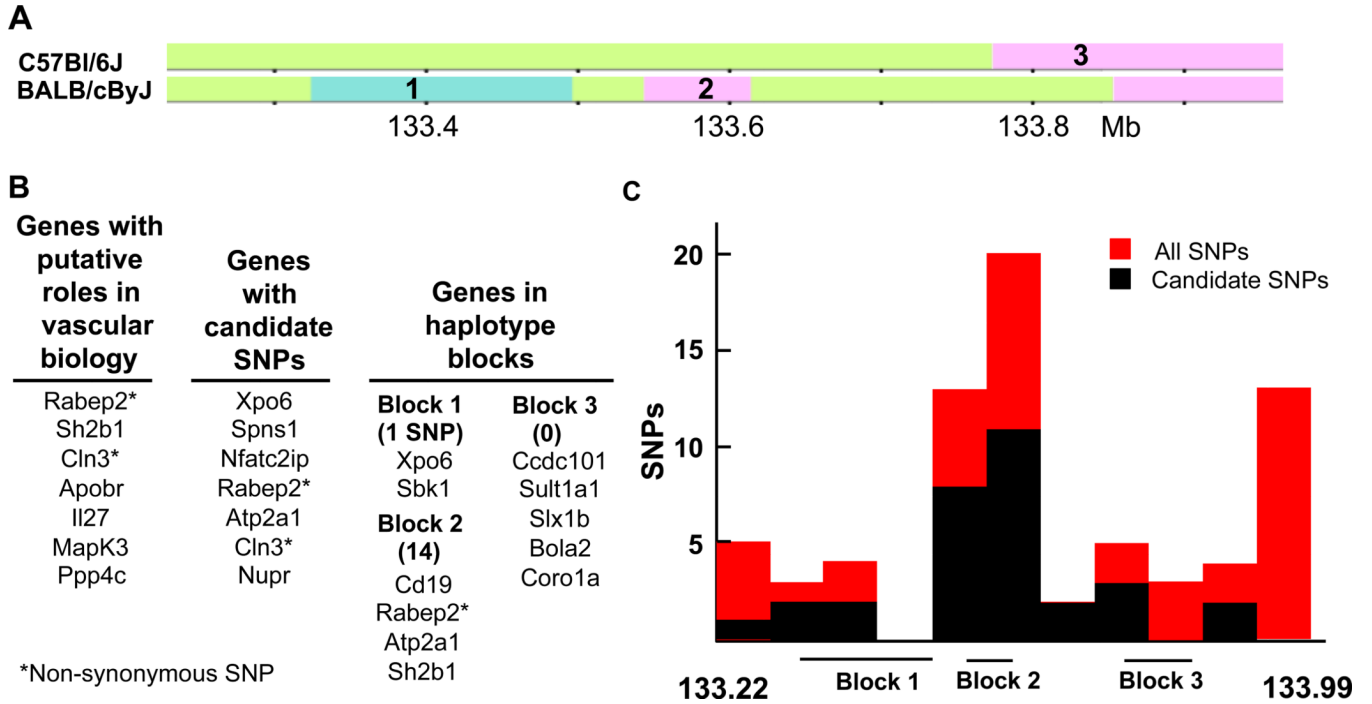


Figure 6. Haplotype, gene and SNP distribution in *Dce1*

A, Haplotype maps of B6 and Bc in *Dce1* from the Mouse Phylogeny Viewer.⁶⁶ Three haplotype blocks contain 11 of the 28 genes and 15 of the 27 candidate SNPs in *Dce1* that distinguish Bc from B6. **B**, Genes within *Dce1* that are involved in vascular biology, harbor candidate SNPs, or occur in haplotype blocks. *Rabep2*, the only gene in all 3 categories, contains 7 candidate SNPs (5 intronic, one synonymous, one non-synonymous) and lies in the small haplotype block number 2 (73 kb) in which lie half of the candidate SNPs in *Dce1*. Numbers in parentheses indicate the number of candidate SNPs in each block. **C**, All SNPs (red bars) and candidate SNPs (black) are unevenly distributed in *Dce1*.